

Wave Propagation in the Photosensitive Belousov–Zhabotinsky Reaction Across an Asymmetric Gap

Takatoshi Ichino,[†] Kenji Fujio,[‡] Mariko Matsushita,[‡] and Satoshi Nakata^{*,§}

Department of Intelligent Systems, School of Biology-Oriented Science and Technology, Kinki University, Wakayama 649-6493, Japan, Department of Chemistry, Nara University of Education, Takabatake-cho, Nara 630-8528, Japan, and Graduate School of Science, Hiroshima University, Kagamiyama 1-3-1, Higashi-Hiroshima 739-8526, Japan

Received: November 11, 2008; Revised Manuscript Received: December 14, 2008

The photosensitive Belousov–Zhabotinsky (BZ) reaction was investigated at an asymmetrically illuminated gap, which was drawn using computer software and then projected on a filter paper soaked with BZ solution using a liquid-crystal projector. The probability of the chemical wave passing through the gap with asymmetric illumination was different from that through its mirror image. The location at which the wave disappeared and the time delay of the chemical wave passing through the gap changed depending on the velocity of chemical wave propagation. The experimental results were qualitatively reproduced by a theoretical calculation based on the three-variable Oregonator model that included photosensitivity. These results suggest that the photosensitive BZ reaction may be useful for studying spatiotemporal development that depends on the geometry of excitable fields.

Introduction

Experimental and theoretical studies on wave propagation in excitable media may help us not only to understand signal processing in biological systems,¹ such as nerve impulses,^{2,3} but also to create novel methods for artificial processing, such as image processing^{4–7} and information processing,^{8–13} based on a reaction-diffusion system. Characteristic features of wave propagation and oscillation on the Belousov–Zhabotinsky (BZ) reaction have been experimentally and theoretically clarified as an excitable or oscillatory chemical system.^{14–16} As an application of the BZ system, there have been many studies on the features of wave propagation in excitable fields with various geometries.^{17–24}

A photosensitive experimental setup for the BZ reaction^{4,5,12,25,26} makes it easier to create excitable fields with various geometries, which are drawn by computer software and then projected on a filter paper soaked with BZ solution using a liquid-crystal projector.^{13,27} In this case, light illumination produces bromine, which inhibits the oscillatory reaction; i.e., the degree of excitability can be adjusted by changing the intensity of illumination. Therefore, the number of chemical waves and their locations can be spatiotemporally regulated by the local illumination of unwanted waves.^{13,28,29} As one of various systems, Tóth et al. reported a numerical model of the photosensitive BZ system that was illuminated asymmetrically as a chemical diode.³⁰ Although the theoretical prediction on the chemical diode was reproduced experimentally as a related experimental system,³¹ the detail features on the chemical diode behavior, e.g., features of hysteresis and wave propagation, have not yet been observed both experimentally and numerically.

In the present study, we examined the characteristic features of wave propagation through a rectangular field with a gap that

was illuminated asymmetrically. The probability of passage of the chemical wave differed between two rectangular fields with gaps that were mirror images of each other. The location at which the wave disappeared and the time delay of the chemical wave passing through the gap changed depending on the velocity of chemical wave propagation. The experimental results were qualitatively reproduced by a theoretical calculation based on the three-variable Oregonator model that included photosensitivity. These results suggest that the photosensitive BZ reaction may be useful for studying spatiotemporal development that depends on the geometry of excitable fields.

Experiments

Ru(bpy)₃Cl₂, purchased from Sigma-Aldrich (St. Louis, MO), was used as a catalyst for the photosensitive BZ reaction. The BZ solution consisted of [NaBrO₃] = 0.47 M, [H₂SO₄] = 0.31 M, [CH₂(COOH)₂] = 0.16 M, [KBr] = 0.01 M, and [Ru(bpy)₃Cl₂] = 1.7 mM. A cellulose nitrate membrane filter (Advantec, A100A025A, diameter of the membrane = 25 mm) with a pore size of 1 μm was homogeneously soaked in BZ solution (5 mL) for about 1 min. The soaked membrane filter was gently wiped with another pure filter paper to remove excess solution and placed on a glass plate (77 × 52 × 1.3 mm³). The surface of the membrane filter was completely covered with 0.7 mL silicone oil (Wako, WF-30) to prevent it from drying and to protect it from the influence of oxygen in air. The experiments were carried out in an air-conditioned room at 298 ± 1 K, at which the reaction medium showed no oscillation and exhibited almost constant wave-propagation behavior for approximately 30 min.

The medium was illuminated from below as shown schematically in Figure 1.²⁹ The high-pressure mercury bulb of a liquid-crystal projector (Mitsubishi, LPV-XL8) was used as a light source, the spatial intensity distribution was controlled with a personal computer, and a magnifying lens was used to adjust the focus. The black and white picture created by the liquid-crystal projector served as an illumination mask to create an

* To whom correspondence should be addressed. Tel. and fax: +81-82-424-7409. E-mail: nakatas@hiroshima-u.ac.jp.

[†] Kinki University.

[‡] Nara University of Education.

[§] Hiroshima University.

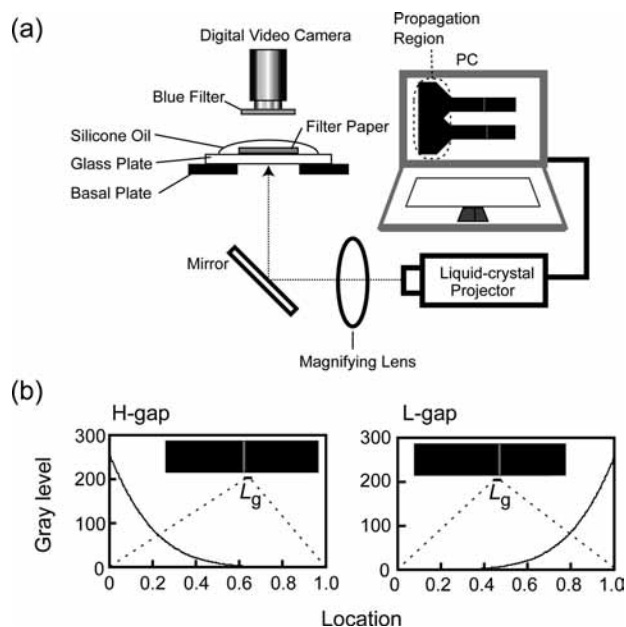


Figure 1. Schematic illustration of (a) the experimental system based on the photosensitive BZ reaction and (b) one-dimensional routes with two asymmetric gaps (H-gap and L-gap) and their spatial gray levels. L_g in (b) is the width of the gap.

appropriate boundary. Two gaps with high-side (H-gap) and low-side entrances (L-gap) were individually introduced on a one-dimensional route and were mirror images of each other (Figure 1). The light intensities on the black and white regions, except for the gap, were 4.0×10^2 and 1.7×10^4 lx, respectively, where the light intensity at the illuminated part was measured with a light intensity meter (Asone, LX-100).

To prepare a unidirectional chemical wave on a one-dimensional route, the following steps were taken. (1) Reaction fields composed of two one-dimensional routes and a propagation region, at which chemical waves originated from the left of the routes, were prepared in an unilluminated reaction field (see "propagation region" in Figure 1). The spatial distributions of the gray level for the gaps in the two one-dimensional routes were mirror images of each other. No chemical wave was observed in the illuminated region. (2) One chemical wave on each one-dimensional route was supplied from the propagation region. (3) To preserve one chemical wave on each one-dimensional route, the excess chemical waves were eliminated under local illumination of the supply side of the one-dimensional route. Thus, we prepared experimental conditions so that one unidirectional chemical wave propagated on each one-dimensional route.

The experiments were monitored from above with a digital video camera (Sony DCR-VX700) and recorded on videotape. A blue optical filter (Asahi Techno Glass, V-42) with a maximum transparency at 410 nm was used to enhance the images of the green-colored chemical waves, which correspond to the oxidized state, $[\text{Ru}(\text{bpy})_3]^{3+}$.

Results

Figure 2 shows (a) snapshots and (b) spatiotemporal plots of wave propagation at H-gap and L-gap at $L_g = 0.9$ mm, where L_g is the length of the gap. Before the chemical waves arrived at the gaps, their velocities were constant at ca. 0.08 mm s^{-1} . For H-gap, the velocity of the chemical wave decreased while it passed through the gap but reverted to the original value after passing through the gap (Figure 2b-1). We define the time lag,

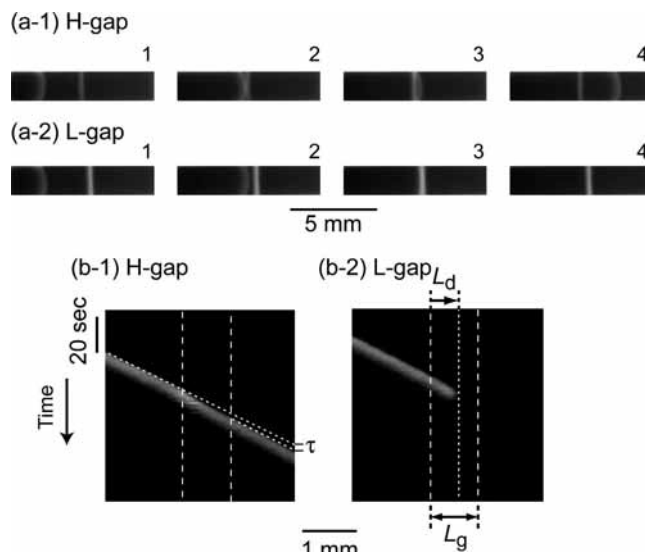


Figure 2. Experimental results: (a) snapshots of wave propagation (top view) and (b) spatiotemporal plots for (1) H-gap and (2) L-gap. The time intervals in (a) were 40 s for 1–2 and 3–4, and 10 s for 2–3. τ in (b-1) is the time lag which is generated by the decrease in the velocity of the chemical wave in the gap, and L_d in (b-2) is the distance from the entrance of the gap to the point at which the chemical wave disappears.

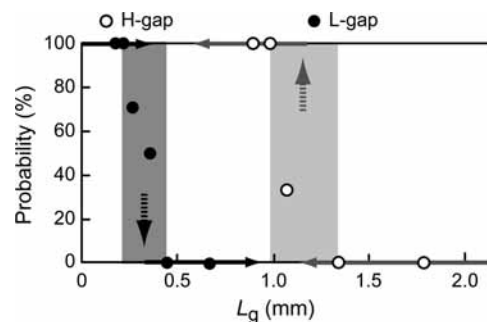


Figure 3. Experimental results for the probability of the passage of a chemical wave through the gap (empty circle, H-gap; filled circle, L-gap) depending on L_g .

τ , to evaluate the decrease in velocity at the gap; i.e., $\tau = t_1 - t_2$, where t_1 and t_2 are the times required for passing through the route with and without a gap. In contrast, for L-gap, the velocity decreased further while the chemical wave passed through the gap, and the wave then disappeared at L_d on the gap (Figure 2b-2), where L_d is the distance from the entrance of the gap to the point at which the wave disappeared.

Figure 3 shows the probability of a chemical wave passing through the gap (empty circle, high-side entrance; filled circle, low-side entrance) depending on the width of the gap. The probabilities were zero when $L_g > 1.0$ mm for H-gap and $L_g > 0.4$ mm for L-gap, i.e., hysteresis that depended on the asymmetry of the gap was observed between $L_g = 0.5$ and 1.0 mm.

Figure 4 shows the experimental results for (a) the time delay (τ) of wave propagation at H-gap versus the velocity of a chemical wave before it entered the H-gap and (b) L_d/L_g versus the velocity of a chemical wave before it entered the L-gap. The velocity decreased with the addition of glycerol at 0–0.04 M to the reaction medium. L_d/L_g was lower than 1; i.e., the chemical wave disappeared in L-gap (see Figure 2b-2). τ decreased but L_d/L_g increased with an increase in the velocity.

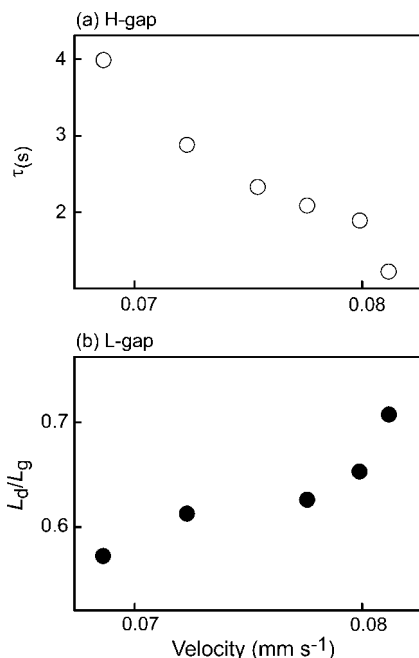


Figure 4. Experimental results for (a) τ versus the velocity of a chemical wave before it enters H-gap and (b) L_d/L_g versus the velocity of a chemical wave before it enters L-gap.

Discussion

We performed numerical calculations based on a three-variable Oregonator modified for the photosensitive BZ reaction and discuss theoretically the mechanism of this phenomenon^{30–33}

$$\frac{\partial u}{\partial t} = f(u, v, w) + D_u \nabla^2 u = \frac{1}{\varepsilon_1} (u - u^2 + qw - uw) + D_u \nabla^2 u \quad (1)$$

$$\frac{\partial v}{\partial t} = g(u, v, w) + D_v \nabla^2 v = u - v + D_v \nabla^2 v \quad (2)$$

$$\frac{\partial w}{\partial t} = h(u, v, w) + D_w \nabla^2 w = \frac{1}{\varepsilon_2} (\phi - qw - uw + \beta v) + D_w \nabla^2 w \quad (3)$$

where u , v , and w are dimensionless variables that correspond to the concentrations of the activator (HBrO_2), the oxidized catalyst ($[\text{Ru}(\text{bpy})_3]^{3+}$), and the inhibitor (Br^-), respectively. $f(u, v, w)$, $g(u, v, w)$, and $h(u, v, w)$ denote the local dynamics on u , v , and w . β , ε_1 , ε_2 , and q are positive parameters that determine the nature of the BZ reaction, D_u , D_v , and D_w are diffusion constants for the activator, the oxidized catalyst, and the inhibitor, respectively, and ϕ is an increasing function of the light intensity. A numerical calculation is performed in one dimension using the Crank–Nicolson implicit method and the Neumann boundary condition. In simulations, we used a one-dimensional grid (n_g) consisting of 10 000 points, and the steps (Δt) for spatial and temporal integration were 0.04 and 0.0001, respectively. The parameters used in the calculations were $f = 2.5$, $\varepsilon_1 = 0.0508$, $\varepsilon_2 = 0.000168$, and $q = 0.0001$. These parameters were chosen to reproduce the experimental results much better, e.g., $L_d/L_g < 1$ and τ depending on the velocity. The spatial distribution of light intensity was constructed with a constant gradient ranging between 0.0007 and 0.02. The gap contained 680 points and was located at the center of the full grid. The chemical wave was initiated by setting the value of u to 0.2 at 3 points at the appropriate boundary. D_u ,

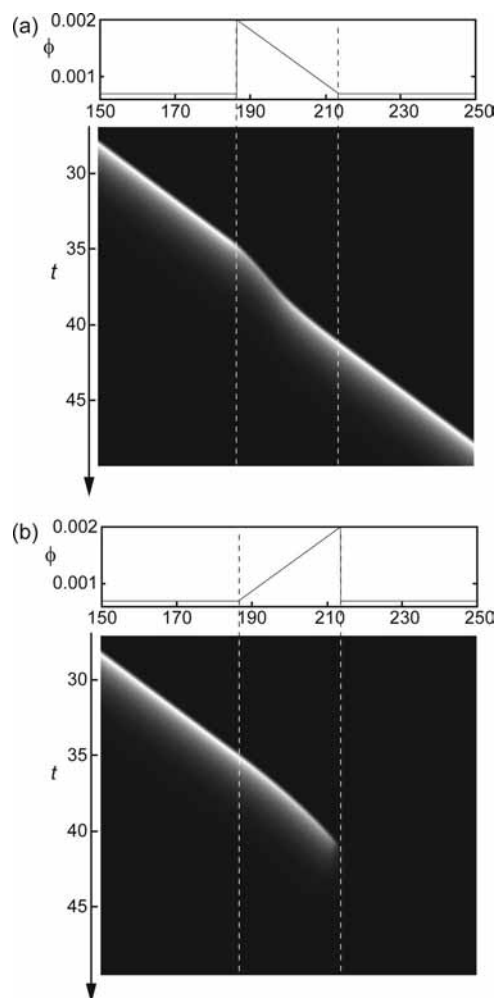


Figure 5. Numerical results of the spatiotemporal plots for (a) H-gap and (b) L-gap. The horizontal axis on the space is $n_g \times \Delta t$. The spatial distribution of ϕ is indicated at the top of the individual plot. The parameters used for H-gap were the same as those for L-gap, and $D_u = D_v = D_w = 1.0$.

D_v , and D_w were equivalent to one another ($D_u = D_v = D_w$), and were varied between 0.95 and 1.05 to change the velocity of wave propagation.

The numerical results regarding the features of wave propagation for H-gap and L-gap based on eqs 1–3 are shown as spatiotemporal plots in Figure 5, and hysteresis on the probability of a chemical wave passing through the gap, either 0 or 1, depending on the width of the gap (L_g), is shown in Figure 6.

Figure 7 shows the numerical results for (a) the time delay (τ) of wave propagation at H-gap versus the velocity of a chemical wave before it enters H-gap and (b) L_d/L_g versus the velocity of a chemical wave before it enters L-gap. Thus, the numerical calculations in Figures 5–7 qualitatively reproduce the experimental observations in Figures 2–4, respectively.

Based on the experimental and numerical results, we discuss the nature of wave propagation via two gaps that are mirror images of each other. Since light illumination produces Br^- due to the photochemical reactions of the catalyst,⁴ the concentration of Br^- in the reaction field under a bright background is higher than that under a dark background, and thus light illumination inhibits the BZ reaction.^{6,26,28}

Hysteresis in the probability of gap passage depending on L_g in Figure 3 may be generated due to the approach condition of

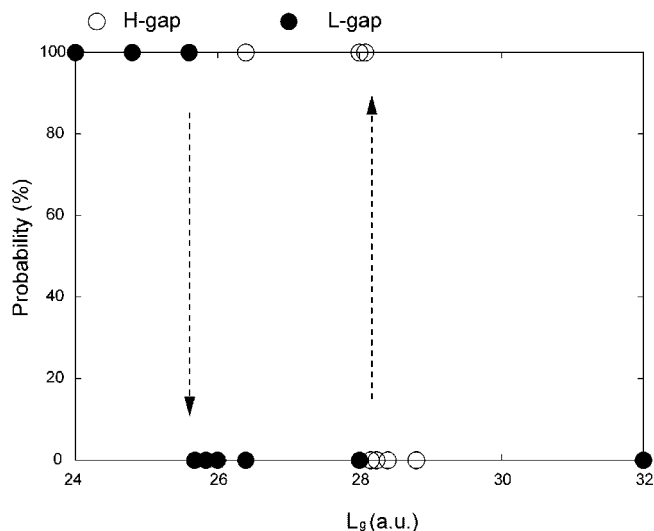


Figure 6. Numerical results for the probability of the passage of a chemical wave through the gap (empty circle, H-gap; filled circle, L-gap) depending on L_g .

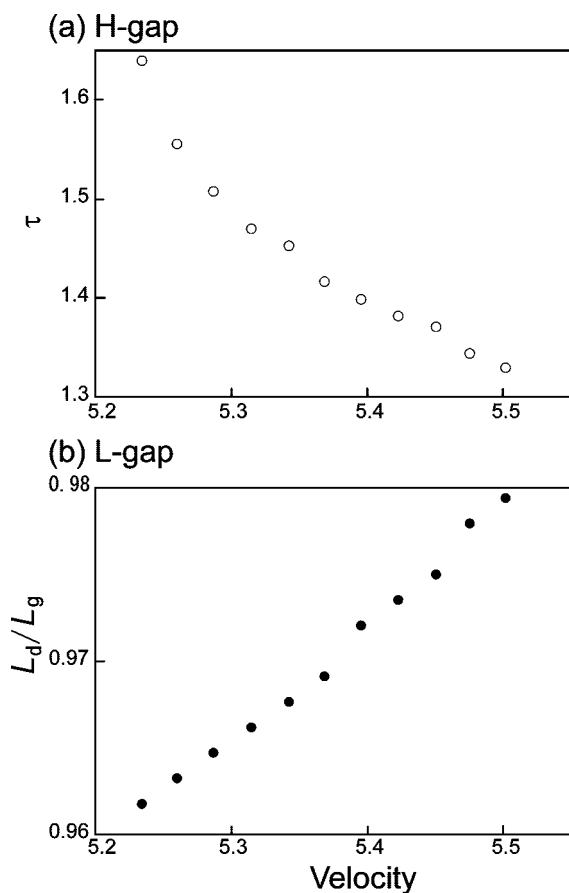


Figure 7. Numerical results for (a) τ versus the velocity of a chemical wave before it enters H-gap and (b) L_d/L_g versus the velocity of a chemical wave before it enters L-gap.

the chemical wave to the region with maximum brightness, which corresponds to the region with the lowest excitability. Since the amplitude and wavelength of the chemical wave decrease before they approach the region with the lowest excitability, the chemical wave is insufficient to maintain wave propagation at L-gap.³⁰ In contrast, the wave entering the region of lowest excitability from the dark area is sufficiently wide to maintain wave propagation at H-gap. In addition, the approach velocity to the region with maximum brightness for L-gap is

lower than that for H-gap, since the velocity for L-gap is decelerated by illumination before it approaches the region.

The dependence of L_d/L_g on the velocity of the chemical wave in Figure 4b may be caused by the passage time of the chemical wave through L-gap. Thus, the passage time for the lower velocity is longer than that for the higher velocity, since a chemical wave with a lower velocity is illuminated for a longer time than a wave with a higher velocity. The velocity dependence of τ in Figure 4a may be discussed similarly by considering the passage time.³⁰

Conclusion

The nature of wave propagation in the photosensitive BZ reaction on an excitable field with the asymmetrically illuminated gap was examined both experimentally and numerically. Hysteresis in the probability of passage of a chemical wave through the gap was observed, i.e., L_g for H-gap was larger than that for L-gap when the probability was zero. With an increase in the velocity of the chemical wave, the time delay (τ) for H-gap decreased and L_d/L_g for L-gap increased. The experimental results can be qualitatively reproduced by a numerical calculation based on the three-variable Oregonator modified for the photosensitive BZ reaction. As for the future work in this system, the stochastic aspect^{34–36} is useful to understand the phenomena. Although the probability in Figure 6 is deterministic in the present simulation, the features of the probability may be changed with the addition of noise.

The photosensitive BZ reaction may be useful for studying spatiotemporal development that depends on the geometric condition of excitable fields, since the shape of the reaction field can be varied using a personal computer. To investigate reaction fields with further complex shapes or to experimentally reproduce theoretical predictions, the development of an experimental system in place of an immersed filter paper will be necessary to maintain and control the features of wave propagation and oscillation at a microlevel.

Acknowledgment. The authors thank Professor Hiroyuki Kitahata (Chiba University, Japan) and Professor Yoshihito Mori (Ochanomizu University, Japan) for their kind suggestions and comments. This work was supported in part by a Grant-in-Aid for Scientific Research (No. 20550124) and by a grant from the Asahi Glass Foundation to S.N.

References and Notes

- (1) Winfree, A. T. *The Geometry of Biological Time*; Springer: Berlin, 1980.
- (2) *Molecular Neurobiology*; Hall, Z. W., Ed.; Sinauer Associates: Sunderland, MA, 1992.
- (3) Murray, J. D. *Mathematical Biology*; Springer: Berlin, 1989.
- (4) Kuhnert, L. *Nature* **1986**, *319*, 393.
- (5) Kuhnert, L.; Agladze, K. I.; Krinsky, V. I. *Nature* **1989**, *337*, 244.
- (6) Rambidi, N. G.; Shamayaev, K. E.; Peshkov, G. Y. *Phys. Lett. A* **2002**, *298*, 375.
- (7) Sakurai, T.; Mihaliuk, E.; Chirila, F.; Showalter, K. *Science* **2002**, *296*, 2009.
- (8) Tóth, A.; Showalter, K. *J. Chem. Phys.* **1995**, *103*, 2058.
- (9) Steinbock, O.; Kettunen, P.; Showalter, K. *J. Phys. Chem.* **1996**, *100*, 18970.
- (10) Motoike, I.; Yoshikawa, K. *Phys. Rev. E* **1999**, *59*, 5354.
- (11) Ichino, T.; Igarashi, Y.; Motoike, N. I.; Yoshikawa, K. *J. Chem. Phys.* **2003**, *118*, 8185.
- (12) Gorecka, J.; Gorecki, J. *Phys. Rev. E* **2003**, *67*, 067203.
- (13) Nagahara, H.; Ichino, T.; Yoshikawa, K. *Phys. Rev. E* **2004**, *70*, 036221.
- (14) Zaikin, A. N.; Zhabotinsky, A. M. *Nature* **1970**, *225*, 535.
- (15) *Oscillations and Traveling Waves in Chemical Systems*; Field, R. J., Burger, M., Eds.; Wiley: New York, 1985.

- (16) *Chemical Waves and Patterns*; Kapral, R., Showalter, K., Eds.; Kluwer Academic: Dordrecht, 1995.
- (17) Lázár, A.; Noszticzius, Z.; Försterling, H.-D.; Nagy-Ungvárai, Z. *Physica D* **1995**, *84*, 112.
- (18) Steinbock, O.; Kettunen, P.; Showalter, K. *Science* **1995**, *269*, 1857.
- (19) Winston, D.; Arora, M.; Masek, J.; Gáspár, V.; Showalter, K. *Nature* **1991**, *351*, 132.
- (20) Iguchi, Y.; Takitani, R.; Miura, Y.; Nakata, S. *Rec. Res. Dev. Pure Appl. Chem.* **1998**, *2*, 113.
- (21) Motoike, N. I.; Yoshikawa, K.; Iguchi, Y.; Nakata, S. *Phys. Rev. E* **2001**, *63*, 036220.
- (22) Agladze, K.; Aliev, R. R.; Yamaguchi, T.; Yoshikawa, K. *J. Phys. Chem.* **1996**, *100*, 13895.
- (23) Aliev, R. R.; Agladze, K. I. *Physica D* **1991**, *50*, 65.
- (24) Yoshida, R.; Takahashi, T.; Yamaguchi, T.; Ichijo, H. *J. Am. Chem. Soc.* **1996**, *118*, 5134.
- (25) Kádár, S.; Amemiya, T.; Showalter, K. *J. Phys. Chem. A* **1997**, *101*, 8200.
- (26) Agladze, K.; Tóth, Á.; Ichino, T.; Yoshikawa, K. *J. Phys. Chem. A* **2000**, *104*, 6677.
- (27) Gorecki, J.; Yoshikawa, K.; Igarashi, Y. *J. Phys. Chem. A* **2003**, *107*, 1664.
- (28) Amemiya, T.; Kádár, S.; Kettunen, P.; Showalter, K. *Phys. Rev. Lett.* **1996**, *77*, 3244.
- (29) Nakata, S.; Morishima, S.; Kitahata, H. *J. Phys. Chem. A* **2006**, *110*, 3633.
- (30) Tóth, Á.; Horváth, D.; Yoshikawa, K. *Chem. Phys. Lett.* **2001**, *345*, 471.
- (31) Gorecka, J. N.; Gorecki, J.; Igarashi, Y. *J. Phys. Chem. A* **2007**, *111*, 885.
- (32) Kádár, S.; Wang, J.; Showalter, K. *Nature* **1998**, *391*, 770.
- (33) Brandstädter, H.; Braune, M.; Schebesch, I.; Engel, H. *Chem. Phys. Lett.* **2000**, *323*, 145.
- (34) Adamatzky, A.; de Lacy Costello, B. *Chaos, Solitons & Fractals* **2007**, *34*, 307.
- (35) Mahara, H.; Yamaguchi, T.; Morikawa, Y.; Amemiya, T.; Yamamoto, T.; Miike, H.; Parmananda, P. *Physica D* **2005**, *205*, 275.
- (36) Yoshimoto, M.; Shirahama, H.; Kurosawa, S. *J. Chem. Phys.* **2008**, *129*, 014508.

JP809955Z